

Performance Analysis of a Pulsejet Engine

Shashank Ranjan Chaurasia¹, Rajesh Gupta² and R.M. Sarviya³

¹ PG student, Department of Mechanical Engineering, Maulana Azad National Institute of Technology Bhopal (M. P.) India

² Associate Professor, Department of Mechanical Engineering, Maulana Azad National Institute of Technology Bhopal (M. P.) India

³ Professor, Department of Mechanical Engineering, Maulana Azad National Institute of Technology Bhopal (M. P.) India

ABSTRACT

This paper investigates the performance of U-type pulsejet engine whose overall length is approximately 160 cm. Gas dynamics, acoustics and chemical kinetics were modeled to gain an understanding of various physical phenomena affecting pulsejet operation, scalability, and efficiency. The pulsejet was run in valveless mode on LPG fuel. Pressure, temperature, thrust, specific impulse, and concentrations of CO, NO and HC at exit of pulse jet engine were measured. Thrust is found to increase with increasing m_f . Concentrations of CO, NO and HC at exit of pulse jet engine were increasing with increasing value of equivalence ratio.

I. Introduction

The pulsejet is one of the simplest propulsion devices requiring no turbo-machinery, or moving parts in some cases. The pulsejet was originally conceived in the early 1900s and developed into a successful propulsion system by the Germans in WWII for the V-1 'buzz bomb', the name being derived from the impressive acoustic emission at 50 Hz from these engines. Their simple structure and light weight make them an ideal thrust-generation device, but their thermodynamic efficiency is low compared to gas turbine engines due to the lack of mechanical compression, which results in low peak pressure. Due to this low efficiency, the pulsejet received little attention after the late 1950s. However, pulsejets with no moving parts may be advantageous for building smaller propulsion devices. The thermodynamic efficiency of conventional engine (such as gas turbines and both SI and CI engine). Decreases non-linearly with decreasing characteristic engine length scale. Also, small scale engines with moving parts are more prone to breakdown due to fatigue of the moving components [1]. Pulsejets, especially valveless pulsejets, are attractive as candidates for miniaturization due to their extremely simple design. The general pulsejet cycle can be illustrated as follows. The combustion event begins when the combustion chamber pressure is above atmospheric and the temperature of the fuel/air mixture increases, due to mixing with residual products, to the auto-ignition temperature. A compression wave is

generated and combustion increases both temperature and pressure in the combustion chamber, driving the flow toward the exit and inlet at gradually increasing velocity. The relatively short combustion event ends and when the compression wave reaches either the pulsejet inlet or the exit, an expansion wave due to overexpansion and travels back into the combustion chamber. Flow velocity reaches its positive maximum at the exit at this time. The expansion wave decreases the pressure in the exhaust tube and the combustion chamber to sub-atmosphere, resulting in backflow at both the inlet and exit. The next charge of air enters into the chamber due to this backflow at the inlet. The mass addition increases the combustion chamber pressure. When the pressure in the combustion chamber approaches the atmosphere pressure, the next cycle begins. One of the most significant and technically challenging aspects of the micro-propulsion device is its limited residence time. Once the combustion chamber size becomes 2–3 orders of magnitude smaller than that of a large scale jet engine, the residence time within the combustion chamber approaches the characteristic chemical kinetic time scale for hydrocarbon–air reactions [2]. In a review paper, Roy et al. [4] reported the typical length for a pulse detonation engine is 0.3–3 m. We believe this 8 cm pulsejet is the smallest operational pulsejet reported [5–8]. The fuel injection system, combustion chamber, and the inlet geometry must be carefully designed to create a fast mixing process and the necessary fluid dynamic and acoustic time scales to permit pulsejet operation.

The fuel injection system, combustion chamber, and the inlet geometry must be carefully designed to create a fast mixing process and the necessary fluid dynamic and acoustic time scales to permit pulsejet operation. Another challenge is the heat loss to the walls due to the high surface-area-to-volume ratio. Large thermal losses have a direct impact on overall combustor efficiency and they can increase kinetic times and narrow flammability limits through suppression of the reaction temperatures [3]. For the oscillating combustion process to be self-sustaining, excessive heat loss, which lowers the temperature of the walls and the residual gas, must be prevented. is generated.

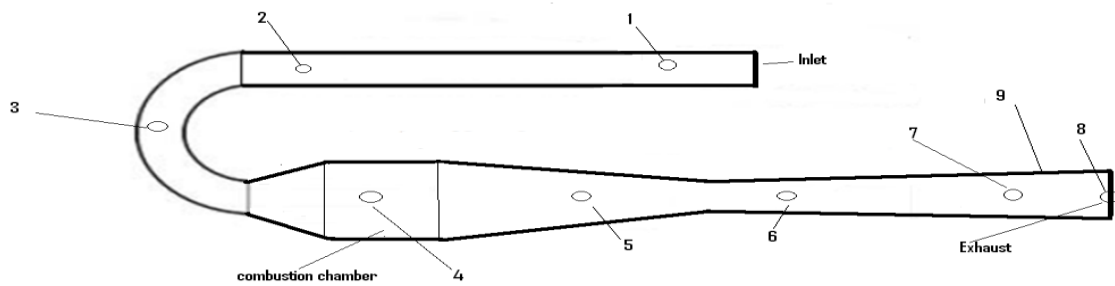


Fig.1.1: Schematic diagram of 160 cm pulse jet engine with different thermocouple position



Fig.1.2: Experimental set up of 160 cm pulse jet engine2.

II. Experimental setup

pulsejet on the order of 160 cm total length have been used for many years for RC aircraft and hydroplane propulsion applications. This version is typically run in a valved mode, with reed valves opening on the low pressure ingestion stroke and closing as the pressure increases due to heat release from combustion. Previously, a 15 cm total length pulsejet was investigated numerically and experimentally [9]. In the 15 cm version, the traditional valved inlet was replaced with a valveless inlet. Attempts to design and build a valved 15 cm pulsejet were unsuccessful due to the reed valves, which were directly scaled down from the 50 cm valves. Furthermore, the reed valves can be easily damaged in the operation of the pulsejet. Thus, we choose valveless designs for 160 cm pulsejets. With the valveless inlets, the inlet cross-sectional area and length were important parameters in determining operability. The current design is based on the 160 cm pulsejets; all dimensions are scaled by half except for the combustion chamber diameter, which is 14 cm. The fuel used in all results reported here was LPG. As opposed to the large valved inlets which use a liquid fuel atomized upstream of the

combustion chamber in a venture and thus only enters the combustion chamber with a fresh charge of air, fuel was injected at a constant rate directly into the combustion chamber. This greatly simplified the fuel injection process and eliminated the need for pulsed injection. The air inflow was still controlled by the oscillating pressure and acoustic waves. The spark igniter can be seen at the top of the pulsejet, shown in Fig. (1.a) and the fuel injection port is parallel to igniter. The combustion chamber was threaded to allow variation in combustion chamber volume, and the exhaust duct was threaded to allow extensions. Mass flow meters were used to measure the fuel flow rate while the air flow rate was not measured (naturally aspirated).

Fast response pressure transducers were used to measure the instantaneous pressure and k-type thermocouples were used to measure average gas temperature inside the jet at various axial locations. Thrust was measured via thrust stand by use of spring deflection.

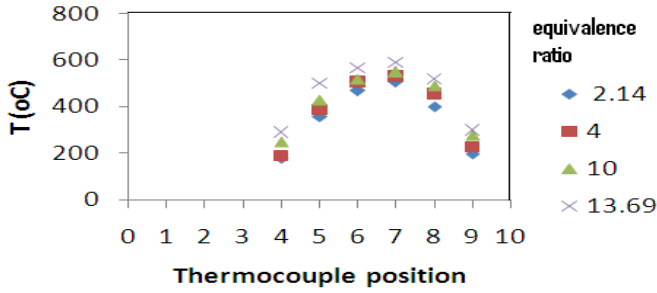


Fig.2: Temperature at different thermocouple position with different equivalence ratio(ϕ).

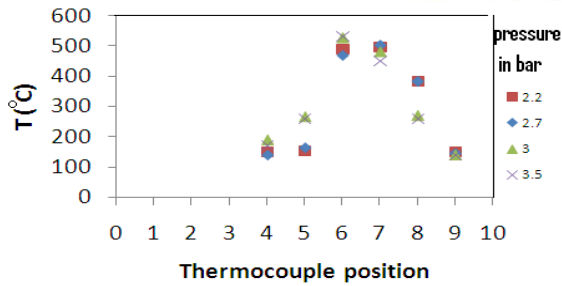


Fig.3: Temperature at different thermocouple position with different combustion chamber pressure.

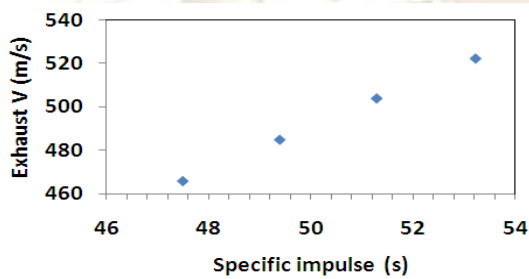


Fig.4: Specific impulse v/s exhaust gas velocity.

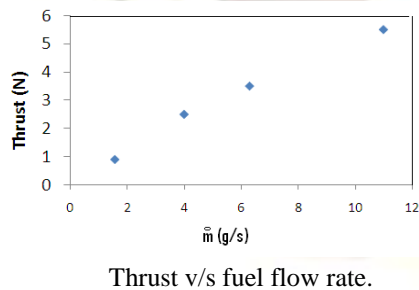


Fig.5:

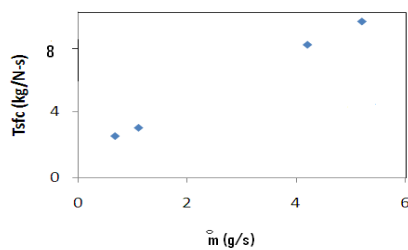


Fig.6: Thrust specific fuel consumption v/s fuel flow rate.

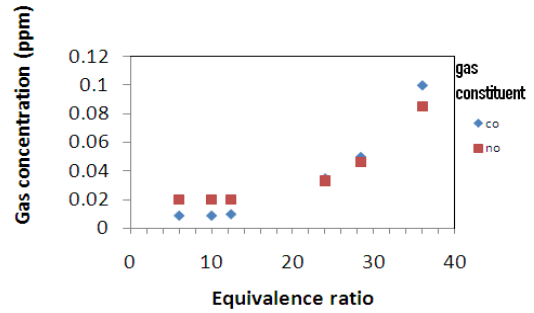


Fig.7: Equivalence ratio v/s concentration of different gas constituent at exhaust.

III. Results and discussion

From the computational results, the pulsejet cycle can be described by the following 10 steps:

1. Combustion event begins when LPG and air mix and are brought to their auto-ignition temperature through mixing with residual hot products from the previous cycle. The pressure and temperature begin to increase in the combustion chamber. Air continues entering the combustion chamber through the inlet with reduced velocity.
2. Combustion continues, and peak pressure and temperature are reached in the combustion chamber. Compression waves are generated and propagate into the inlet and the exhaust tube. When the pressure of the hot gases becomes equal to the pressure of the cold air, the velocity goes to zero at the interface of these two gases.
3. Expansion waves are generated at the inlet and decrease pressure in the combustion chamber. A positive, increasing velocity characterizes the flow at the exhaust duct exit; while at the inlet, the hot products are expelled with an increasing (negative) velocity.
4. Expansion waves are generated at the exhaust duct exit and travel back to the combustion chamber. Pressure decreases in the combustion chamber and the gas velocity out of the inlet and the exit reach their maximum. Most of LPG is burned by this stage.
5. The pressure in the combustion chamber continues decreasing. Temperature increases in the inlet.
6. Expansion waves from the exit enter the combustion chamber and further decrease the pressure in the combustion chamber. The outgoing (negative) velocity at the inlet decreases to zero.
7. The combustion chamber pressure decreases below atmospheric, causing air to enter the combustion chamber through the inlet. Hot products continue to be expelled from the exhaust duct exit but the velocity continuously decreases.
8. The pressure and temperature in the combustion chamber continue decreasing while the inlet velocity continues increasing. The product velocity at the

exhaust duct exit goes to zero and then actually reverses. This backflow causes a temperature drop due to entrainment of ambient air up the exhaust duct.

9. Cold air from the inlet continually enters the combustion chamber. Hot gas in the exhaust duct is pushed back to the combustion chamber. The pressure in the combustion chamber continues to increase.

10. Backflow continues, but its negative velocity becomes smaller. When the pressure in the combustion chamber approaches atmospheric pressure and air from the inlet mixes with LPG in the combustion chamber, the next cycle begins.

It was observed that chemical reaction consumes most of the oxygen in the combustion chamber. The oxygen that is needed for the combustion comes from the inlet only. The inlet design determines the amount of air entering the combustion chamber and thus plays a significant role in valveless pulsejet performance.

3.1. Peak combustion chamber pressure

In this paper, peak pressure is used as an engine performance metric. The majority of the tests in pulsejet were conducted at a continuous fuel flow rate, \dot{m}_f , of 9 g/s of LPG. However, the pulsejet will operate over a rather large range of fuel flow rates.

This particular pulsejet will operate with fuel flows as low as 3 g/s and as high as 12 g/s of LPG. At \dot{m}_f values beyond these limits, the jet extinguishes itself and can no longer sustain its operation. Fig. 2 shows how the pulsejet's instantaneous combustion chamber pressure responds to changes in \dot{m}_f . At 3 mg/s, the pulsejet is barely operating in the pulsejet mode, as is indicated by a very small pressure rise. Also, a higher frequency event was clearly observed at the low end of the \dot{m}_f range. As \dot{m}_f is increased, the secondary pressure spike decreases in magnitude, and is barely detectable when \dot{m}_f is 10 g/s. The operating frequency of the jet varies with fuel flow rate only at the low end. Once \dot{m}_f reaches 6 g/s, the frequency of the pulsejet remains relatively constant. This can be observed audibly as well: when the pulsejet first starts at the lowest fuel setting, it sounds slightly different than the high-pitched hum that accompanies the jet at full throttle. Fig. 2 shows a summary of experiments conducted comparing the jet's behavior at various \dot{m}_f . Based solely on these pressure traces, it is assumed that the jet operates most efficiently at the point of highest frequency and peak pressure—somewhere between 7 and 10 g/s.

In contrast to the forward-facing inlet, the throttle ability of the pulsejet changes considerably. The operating range of the jet lies roughly between 6 g/s and 9 g/s of LPG. The jet will not start outside

these \dot{m}_f values, and varying \dot{m}_f outside these values once the jet has started results in the jet cutting off. This decrease in throttle ability is most likely the result of poor mixing conditions for the rearward-facing inlets. The pulsejet is able to ingest a much wider range of air flow in the forward-facing configuration, enabling the pulsejet to operate over a wider range of \dot{m}_f . Fig. 2 shows a summary of the pressure traces of the pulsejet in the rearward configuration at various \dot{m}_f . As with the forward-facing configuration, the frequency steadily increases with increasing \dot{m}_f . This can be observed audibly in the experiments. In contrast to Fig. 3 the peak pressure rise quickly reaches a steady value as the fuel flow rate is increased. The inlet configuration does not allow the pulsejet to breathe as easily, thus the pulsejet shuts off at a lower fuel setting.

3.2. Net thrust and fuel consumption

It was demonstrated through exhaust velocity measurements in the 160 cm pulsejet that the exhaust cycles between positive and negative velocities in a sinusoidal fashion [10]. This negative exit velocity results in negative thrust for some portion of the oscillating period. Thus, time-resolved thrust measurements were desirable to investigate how the pulsejet's thrust is coupled to combustion chamber pressure. It was expected that the resultant net thrust should be very small due to the expelling of combustion products. The time-resolved thrust of the 160 cm pulsejet in the forward-facing inlet configuration. It can be seen from this figure that the average thrust is indeed very small. The thrust oscillation frequency appears to be double that of the pressure trace, although this may be an artifact of the thrust stand, whose natural frequency was only a factor of three higher. As the pressure begins to fall below atmospheric, the pulsejet appears to produce a sudden burst of positive thrust. In the rearward configuration, all of the products from the combustion chamber are being expelled in the same direction. During the sub-atmospheric air ingestion phase, the momentum flux occurs in the opposite direction and produces a negative thrust component. However, this component is small when compared with the positive component of the exhaust flow due to its much lower velocity. Fig. 5 shows the time history of the pulsejet's thrust. The thrust curve has an average thrust of 0.95 N, yielding a thrust specific fuel consumption of 1.1g/N-s. The thrust measurements are at a frequency that is twice that of the pressure trace. However, no negative thrust was observed in the rearward inlet configuration.

IV. Conclusions

Valveless pulsejets may be good candidates for propulsion devices due to their simple designs. A

combined experimental and numerical approach was used to investigate the performance of a LPG fueled 160 cm valveless pulsejet. To the author's knowledge, this is the smallest operational pulsejet reported. This work showed that:

1. The Experiment provided physical insight into the pulsejet operation. It was observed that for each operational cycle, combustion consumes most of the oxygen in the combustion chamber, and the oxygen comes from the inlet only. Acoustics and fluid mechanics are both important in determining the operating characteristics of these engines.
2. In the traditional valved inlet, the operating frequency is solely a function of the jet length. However, in valveless mode, the operating frequency is also a function of inlet length, but does not act as a 1/4 wave tube. Rather, the frequency scales with the inlet length raised to negative 0.22 power.
3. The operating frequency and peak pressure rise are a function of $\dot{m}f$. At low $\dot{m}f$, both frequency and pressure are low and increase with increasing $\dot{m}f$. the frequency and pressure both have a maximum, the frequency continues to increase until the maximum $\dot{m}f$ is reached. The pressure reaches a maximum at lower $\dot{m}f$, but does not decrease as $\dot{m}f$ continues to increase.
4. the net thrust is very low as expected., the net thrust improves to approximately 5 N, resulting in a TSFC of 1.1 g/N-s.

References

- [1] A. Majumdar, C. Tien, *Microscale Thermophys. Eng.* 2 (1998) 67–69.
- [2] I.A. Waitz, G. Gauba, Y. Tzeng, *Fluids Eng.* 120 (1998) 109–117.
- [3] C.M. Spadaccini, A. Mehra, J. Lee, X. Zhang, S. Lukachko, I.A. Waitz, *Eng. Gas Turbines Power* 125 (2003) 709–719.
- [4] G.D. Roy, S.M. Frolov, A.A. Borisov, D.W. Netzer, *Prog. Energy Combust. Sci.* 6 (2004) 545–672.
- [5] S. Eidelman, W. Grossman, I. Lottati, J. *Propulsion Power* 7 (6) (1991) 857–865.
- [6] W. Fan, C. Yan, X. Huang, Q. Zhang, L. Zheng, *Combust. Flame* 133 (2003) 441450.
- [7] T.R.A. Bussing, G. Pappas, AIAA-94-0263, January 1994.
- [8] K. Kailasanath, AIAA-2002-0470, January 2002.
- [9] T. Geng, M.A. Schoen, A.V. Kuznetsov, W.L. Roberts, *Flow Turbulence Combust.*, in press.
- [10] T. Geng, A. Kiker, R. Ordon, M.A. Schoen, A.V. Kuznetsov, T. Scharon, W.L. Roberts, 4th Joint Meeting of the US

Sections of the Combust. Institute, Philadelphia, 2005.

- [11] C.K. Westbrook, F.L. Dryer, *Combust. Sci. Technol.* 27 (1981) 31–43.
- [12] H. Tsien (Ed.), *Jet Propulsion*, Guggenheim Aero. Lab., 1946